High-Q^2 e^+p Neutral Current Cross Sections at HERA and Determination of the Structure Function $x\tilde{F}_3$

Friederike Januschek
DESY

On Behalf of the ZEUS Collaboration

DIS 2012, 26-30 March, Bonn, Germany

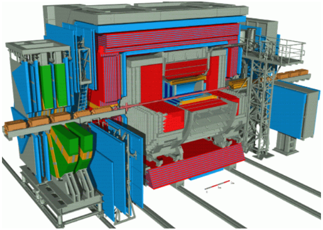

1. Polarised Cross Sections
2. Unpolarised Cross Sections
   - $x\tilde{F}_3$ extraction

The HERA Collider

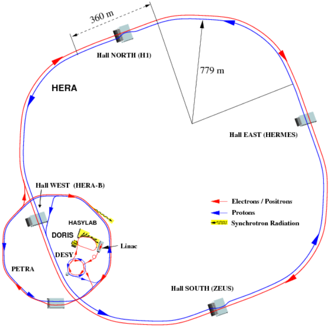

Integrated luminosity:
$0.5\ \mathrm{fb}^{-1}$ per experiment
ZEUS and H1

- HERA: electron-proton collider with $\sqrt{s} = 318\ \mathrm{GeV}$

27.5 GeV 920 GeV

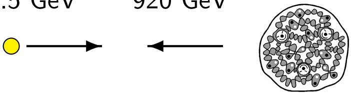

- Four experiments: HERA B, HERMES; H1 and ZEUS
- Two data-taking periods: HERA I (92-00) and HERA II (03-07)
- HERA-II: longitudinally polarised lepton beam

The ZEUS Detector

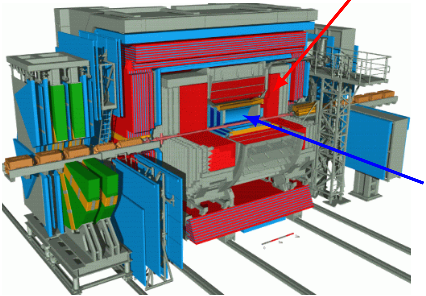

Uranium-Scintillator Calorimeter

Energy and position of particles

- covering 99.7 % of the solid angle
- electromagnetic CAL: $\frac{\sigma_{\mathrm{em}}(E)}{E} = \frac{18\%}{\sqrt{E}}$
- hadronic CAL: $\frac{\sigma_{\mathrm{had}}(E)}{E} = \frac{35\%}{\sqrt{E}}$

Tracking System

Direction and momentum of charged particles

- CTD: cylindric drift chamber (length: 241 cm, $0.3 < \theta < 2.85$)
- MVD: silicon strip detector

Deep Inelastic Scattering

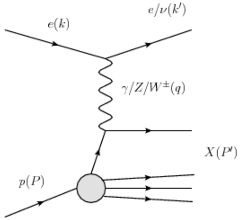

- Neutral Current (NC), γ or Z exchange.
  $e^{\pm}p \rightarrow e^{\pm}X$
- Charged Current (CC), $W^{\pm}$ exchange.
  $e^{\pm}p \rightarrow \nu X$

Variables which characterise DIS:

- Q^2 probing power, negative 4-momentum squared:
  $Q^2 = -q^2 = -(k - k^{`})$
- Bjorken x, momentum fraction of proton carried by struck quark:
  $x = Q^2/2P \cdot q$
- Inelasticity y:
  $y = P \cdot q/P \cdot k$
- s is the centre-of-mass energy squared:
  $s = (P + k)^2$
- These are related by:
  $Q^2 = sxy$

Neutral Current Events in the ZEUS Detector

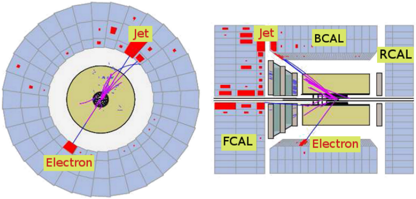

- Well measured scattered $e^{\pm}$.
- $e^{\pm}$ energy deposits and jet(s) balanced in ϕ.
- Kinematics may be reconstructed in multiple ways.

Proton Structure Functions

$$\frac{d^2\sigma_{NC}^{e^\pm p}}{dxdQ^2} = \frac{2\pi\alpha^2}{xQ^4}\left[\underbrace{Y_+\tilde{F}_2(x,Q^2)}_{\text{dominant}} \mp \underbrace{Y_- x\tilde{F}_3(x,Q^2)}_{\text{relevant at high } Q^2} - \underbrace{y^2\tilde{F}_L(x,Q^2)}_{\text{relevant at high } y}\right]$$

where $Y_\pm = 1 \pm (1-y)^2$

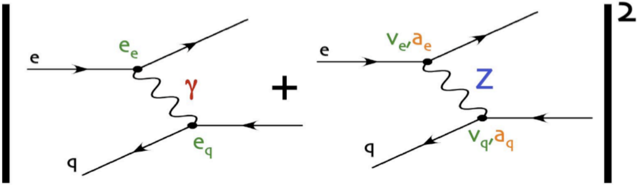

Proton Structure Functions

$$\frac{d^2\sigma_{NC}^{e^\pm p}}{dxdQ^2} = \frac{2\pi\alpha^2}{xQ^4}\left[\underbrace{Y_+\tilde{F}_2(x,Q^2)}_{\text{dominant}} \mp \underbrace{Y_- x\tilde{F}_3(x,Q^2)}_{\text{relevant at high } Q^2} - \underbrace{y^2\tilde{F}_L(x,Q^2)}_{\text{relevant at high } y}\right]$$

$$\tilde{F}_2^{\pm} = F_2^{\gamma} - (v_e \mp P_e a_e)\chi_Z F_2^{\gamma Z} + (v_e^2 + a_e^2 \mp 2\overbrace{P_e}^{\text{polarisation of } e} v_e a_e)\chi_Z^2 F_2^Z$$

$$x\tilde{F}_3^{\pm} = -(\underbrace{a_e}_{\text{axial-vector coupling of } e \text{ to } Z} \mp P_e v_e)\chi_Z xF_3^{\gamma Z} + (\mp P_e(v_e^2 + a_e^2) + 2\underbrace{v_e}_{\text{vector coupling of } e \text{ to } Z} a_e)\chi_Z^2 xF_3^Z$$

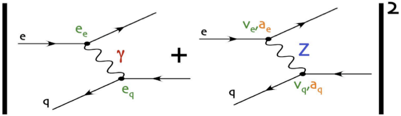

Proton Structure Functions

$$\frac{d^2\sigma^{e^\pm p}_{NC}}{dxdQ^2} = \frac{2\pi\alpha^2}{xQ^4}\left[\underbrace{Y_+\tilde{F}_2(x,Q^2)}_{\text{dominant}} \mp \underbrace{Y_- x\tilde{F}_3(x,Q^2)}_{\text{relevant at high } Q^2} - \underbrace{y^2\tilde{F}_L(x,Q^2)}_{\text{relevant at high } y}\right]$$

$$\tilde{F}_2^\pm = F_2^\gamma - (v_e \mp P_e a_e)\chi_Z F_2^{\gamma Z} + (v_e^2 + a_e^2 \mp 2\overbrace{P_e}^{\text{polarisation of } e} v_e a_e)\chi_Z^2 F_2^Z$$

$$x\tilde{F}_3^\pm = -(\underbrace{a_e}_{\text{axial-vector coupling of } e \text{ to } Z} \mp P_e v_e)\chi_Z xF_3^{\gamma Z} + (\mp P_e(v_e^2 + a_e^2) + 2\underbrace{v_e}_{\text{vector coupling of } e \text{ to } Z} a_e)\chi_Z^2 xF_3^Z$$

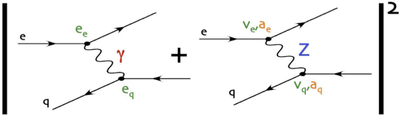

Proton Structure Functions

$$\frac{d^2\sigma_{NC}^{e^\pm p}}{dxdQ^2} = \frac{2\pi\alpha^2}{xQ^4}\left[\underbrace{Y_+\tilde{F}_2(x,Q^2)}_{\text{dominant}} \mp \underbrace{Y_- x\tilde{F}_3(x,Q^2)}_{\text{relevant at high } Q^2} - \underbrace{y^2\tilde{F}_L(x,Q^2)}_{\text{relevant at high } y}\right]$$

$$\tilde{F}_2^{\pm} = F_2^{\gamma} - (v_e \mp P_e a_e)\chi_Z F_2^{\gamma Z} + (v_e^2 + a_e^2 \mp 2\overbrace{P_e}^{\text{polarisation of } e} v_e a_e)\chi_Z^2 F_2^{Z}$$

$$x\tilde{F}_3^{\pm} = -(\underbrace{a_e}_{\text{axial-vector coupling of } e \text{ to } Z} \mp P_e v_e)\chi_Z xF_3^{\gamma Z} + (\mp P_e(v_e^2 + a_e^2) + 2\underbrace{v_e}_{\text{vector coupling of } e \text{ to } Z} a_e)\chi_Z^2 xF_3^{Z}$$

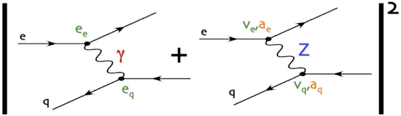

Proton Structure Functions

$$\frac{d^2\sigma_{NC}^{e^\pm p}}{dxdQ^2} = \frac{2\pi\alpha^2}{xQ^4}\left[\underbrace{Y_+\tilde{F}_2(x,Q^2)}_{\text{dominant}} \mp \underbrace{Y_- x\tilde{F}_3(x,Q^2)}_{\text{relevant at high } Q^2} - \underbrace{y^2\tilde{F}_L(x,Q^2)}_{\text{relevant at high } y}\right]$$

$$\tilde{F}_2^\pm = F_2^\gamma - (v_e \mp P_e a_e)\chi_Z F_2^{\gamma Z} + (v_e^2 + a_e^2 \mp 2\overbrace{P_e}^{\text{polarisation of } e} v_e a_e)\chi_Z^2 F_2^Z$$

$$x\tilde{F}_3^\pm = -(\underbrace{a_e}_{\text{axial-vector coupling of } e \text{ to } Z} \mp P_e v_e)\chi_Z xF_3^{\gamma Z} + (\mp P_e(v_e^2 + a_e^2) + 2\underbrace{v_e}_{\text{vector coupling of } e \text{ to } Z} a_e)\chi_Z^2 xF_3^Z$$

- $[F_2^\gamma, F_2^{\gamma Z}, F_2^Z] = \sum_q [e_q^2, 2e_q v_q, v_q^2 + a_q^2] x(q + \bar{q})$
- $[xF_3^{\gamma Z}, xF_3^Z] = \sum_q [e_q a_q, v_q a_q] x(q - \bar{q})$
- $\tilde{F}_L \approx \frac{\alpha_s}{8.3} xg$

Importance of High-Q^2 NC Measurements

- The NC cross sections are a powerful probe of the parton distributions (PDFs).
- The NC cross sections are sensitive to all flavours.
- The difference between the e^+p and e^-p NC cross sections gives direct access to the structure function $x\tilde{F}_3$.
- The longitudinal polarisation asymmetry, $A^+ \approx a_e v_q$ allows parity violation to be directly measured.

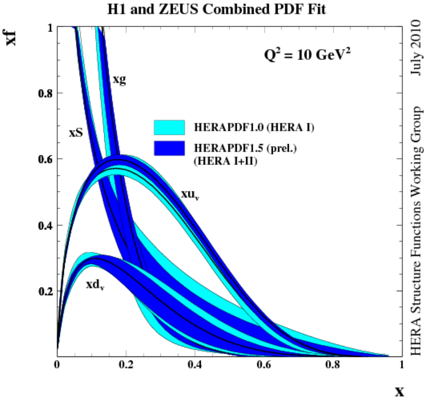

HERA and the LHC

- HERA has a large kinematic reach.
- HERA PDFs can be extrapolated into the LHC region (DGLAP evolution).
- HERA data crucial for calculations of measurements and new physics at the LHC.

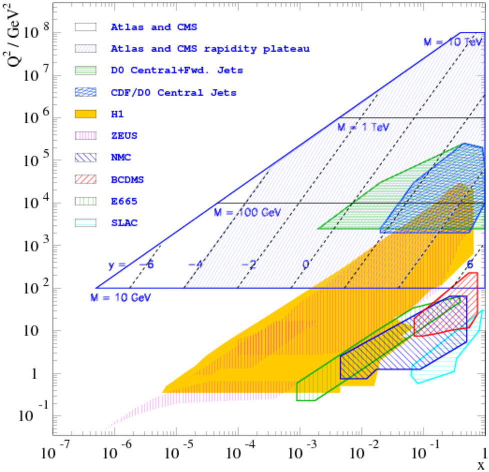

Neutral Current Sample (e^+p Data)

- ZEUS-prel-11-003.
  - This data completes the HERA-II ZEUS high-Q^2 inclusive analyses.

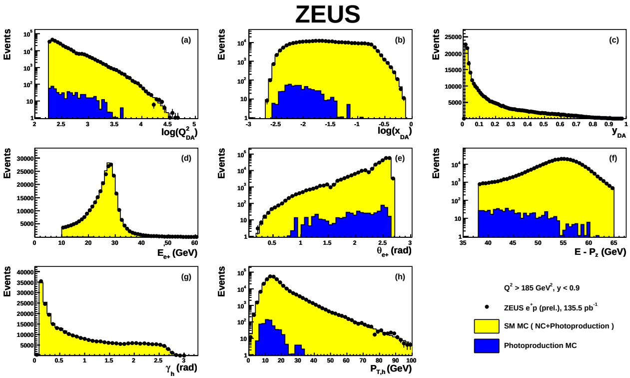

- e^+p data, taken 2006-07, $\mathcal{L} = 135\ \mathrm{pb}^{-1}$
  - $P_e = +32\%$, $\mathcal{L} = 78.8\ \mathrm{pb}^{-1}$
  - $P_e = -36\%$, $\mathcal{L} = 56.7\ \mathrm{pb}^{-1}$
- Kinematic range: $Q^2 > 185\ \mathrm{GeV}$ and $y < 0.9$.
- Data well described.

$d\sigma/dx$ and $d\sigma/dy$ with $P_e > 0$ and $P_e < 0$

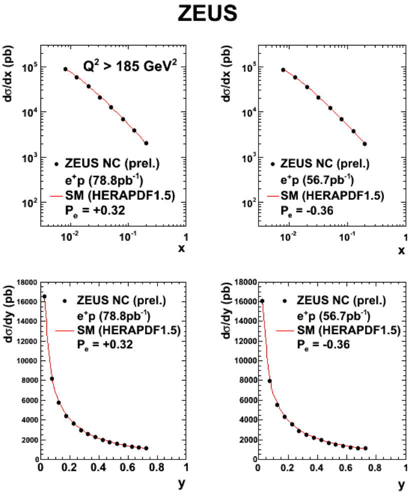

$d\sigma/dx$ and $d\sigma/dy$ with $P_e > 0$ and $P_e < 0$

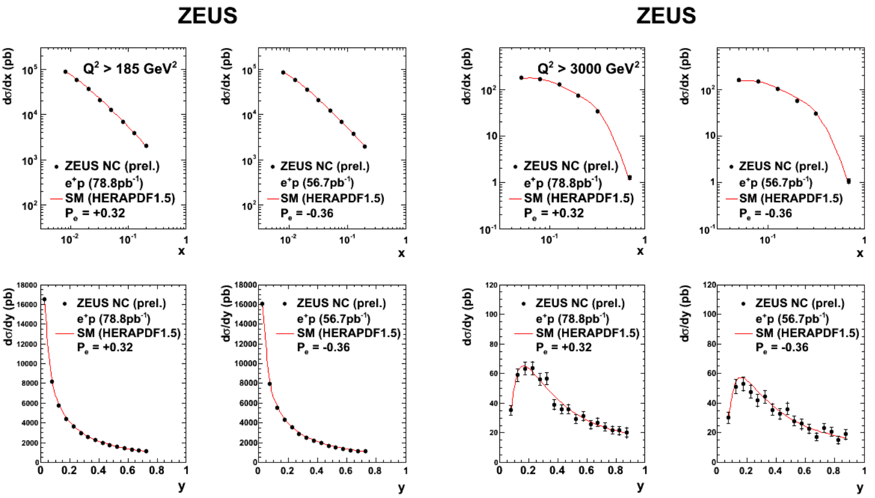

$d\sigma/dQ^2$ with $P_e > 0$ and $P_e < 0$

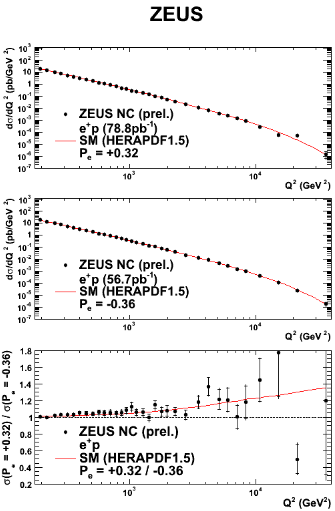

- The difference between the two polarisation states clearly seen at higher-Q^2.

← RH: $d\sigma/dQ^2$ with positive P_e.

← LH: $d\sigma/dQ^2$ with negative P_e.

← RH/LH: ratio of cross sections with positive P_e/negative P_e.

- These results are not included in the shown SM expectation (HERAPDF1.5).

Asymmetry

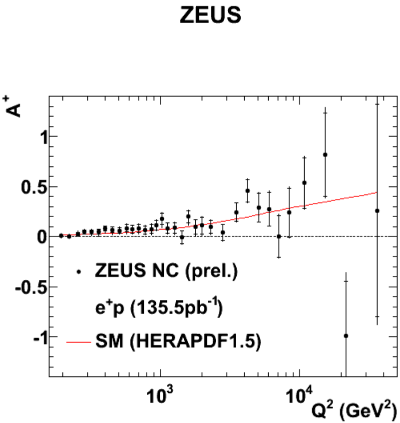

$$A^+ = \frac{2}{P_+ - P_-} \frac{\sigma^+(P_+) - \sigma^+(P_-)}{\sigma^+(P_+) + \sigma^+(P_-)}$$

- $A^+ \approx a_e \chi_Z \frac{F_2^{\gamma Z}}{F_2^{\gamma}} = a_e \chi_Z \frac{2 e_q v_q}{e_q^2} \propto a_e v_q$
- A^+ sensitive to v_q.
- A^+ increases with Q^2.

$\tilde{\sigma}$ with $P_e > 0$ and $P_e < 0$

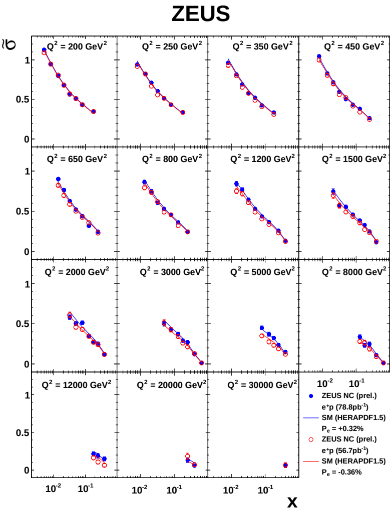

- Closed circles → positive P_e.
- Open circles → negative P_e.
- Effect of polarisation visible at high-Q^2.

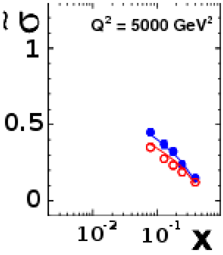

$d\sigma/dQ^2$, $d\sigma/dx$ and $d\sigma/dy$ with P_e=0

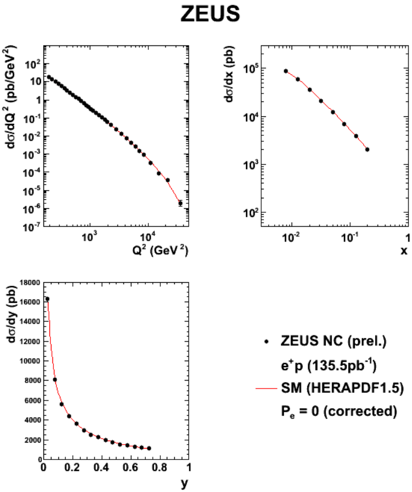

- Measurement over large kinematic ranges.
- The results will help further constraining the PDFs.

$\tilde{\sigma}$ with $P_e = 0$ for e^+p and e^-p

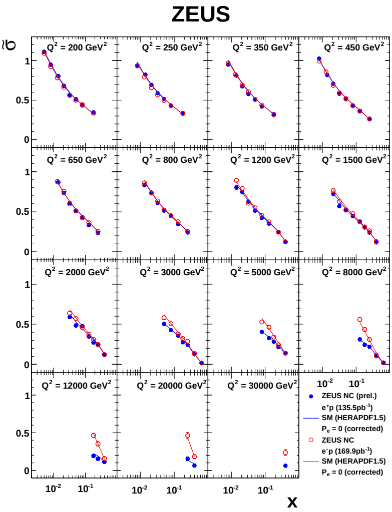

- Closed circles → Full e^+p data set.
- Open circles → Previously measured unpolarised e^-p $\tilde{\sigma}$.
- Difference between e^+p and e^-p clearly seen.
  - Described well by SM predictions.

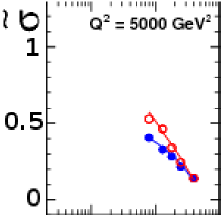

$x\tilde{F}_3$ Extraction

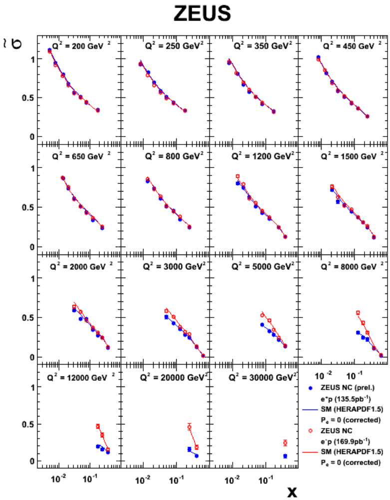

- $\tilde{\sigma}^{e^{\pm}p} = \frac{xQ^4}{2\pi\alpha^2}\frac{1}{Y_+}\frac{d^2\sigma^{e^{\pm}p}_{NC}}{dxdQ^2} = \tilde{F}_2(x,Q^2) \mp \frac{Y_-}{Y_+} x\tilde{F}_3(x,Q^2) - \frac{y^2}{Y_+}\tilde{F}_L(x,Q^2)$
- Difference of e^+p and e^-p $\Rightarrow x\tilde{F}_3$-extraction.
- Expected to contribute at high-Q^2.

$x\tilde{F}_3$ Extraction

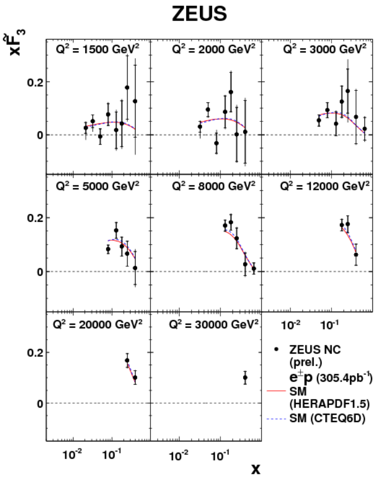

- 135.5 pb^{-1} e^+ data and 169.9 pb^{-1} e^-p data combined to extract $x\tilde{F}_3$.
- Difference between e^+p and e^-p gives xF_3.

$$x\tilde{F}_3(x, Q^2) = \frac{Y_+}{2Y_-}\left(\tilde{\sigma}^{e^-p} - \tilde{\sigma}^{e^+p}\right)$$

$x\tilde{F}_3$ Extraction

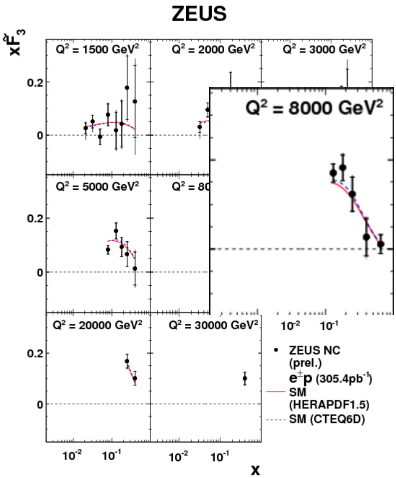

- 135.5 pb^{-1} e^+ data and 169.9 pb^{-1} e^-p data combined to extract $x\tilde{F}_3$.
- Difference between e^+p and e^-p gives xF_3.

$$x\tilde{F}_3(x, Q^2) = \frac{Y_+}{2Y_-}\left(\tilde{\sigma}^{e^-p} - \tilde{\sigma}^{e^+p}\right)$$

- Most precise $x\tilde{F}_3$ measurement.

Summary

- Both the single differential and reduced NC e^+p cross sections have been precisely measured for right- and left-handed polarisation.
- This data completes the ZEUS HERA-II High-Q^2 inclusive data.
- Effects of polarisation are clearly visible in the e^+p data.
- Through the polarisation asymmetry parity violation has been directly measured.
- $x\tilde{F}_3$ was extracted$\longrightarrow$ measurement of the valence quarks
- Data will help in better constraining the PDFs.

BACKUP

Luminosity and Polarisation

- Luminosity measurement through Bethe-Heitler process $ep \to e' p\gamma$
- Two independent measurements by *Photon Calorimeter and Spectrometer*
- Precision: 1.8%
- For this analysis: $\mathcal{L}_{\rm Int} = 135.5\rm{pb}^{-1}$

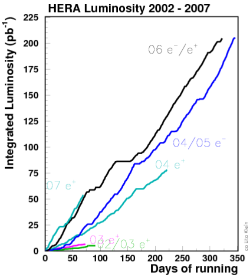

- Spin rotators to get longitudinal polarisation
- Two independent polarisation measurements
- For 2006/07 e^+p:
  $P_e(RH) \approx +0.32$
  ($\mathcal{L}_{\rm Int}$ =78.8 pb^{-1}) and
  $P_e(LH) \approx -0.36$

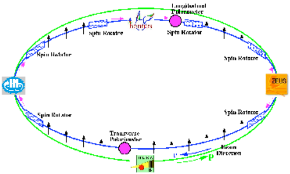

Reconstruction of Variables - Double-Angle Method

- The polar angles of the electron and the hadronic system are used for the reconstruction of the kinematic variables (γ_{had}, θ_e).
- Result does not depend on the absolute calorimeter energy measurement in the detector.
- Best-suited two-variable method.

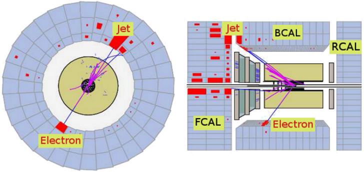

Reconstruction of Variables - Double-Angle Method

- The polar angles of the electron and the hadronic system are used for the reconstruction of the kinematic variables (γ_{had}, θ_e).
- Result does not depend on the absolute calorimeter energy measurement in the detector.
- Best-suited two-variable method.

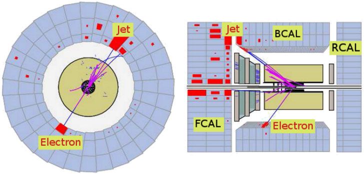

$$Q^2_{DA} = E_e^2 \frac{\sin(\gamma_{had})(1+\cos(\theta_e))}{\sin(\gamma_{had})+\sin(\theta_e)-\sin(\gamma_{had}+\theta_e)}$$

$$x_{DA} = \frac{E_e}{E_p} \cdot \frac{\sin(\gamma_{had})+\sin(\theta_e)+\sin(\gamma_{had}+\theta_e)}{\sin(\gamma_{had})+\sin(\theta_e)-\sin(\gamma_{had}+\theta_e)}$$

$$y_{DA} = \frac{\sin(\theta_e)(1-\cos(\gamma_{had}))}{\sin(\gamma_{had})+\sin(\theta_e)-\sin(\gamma_{had}+\theta_e)}$$